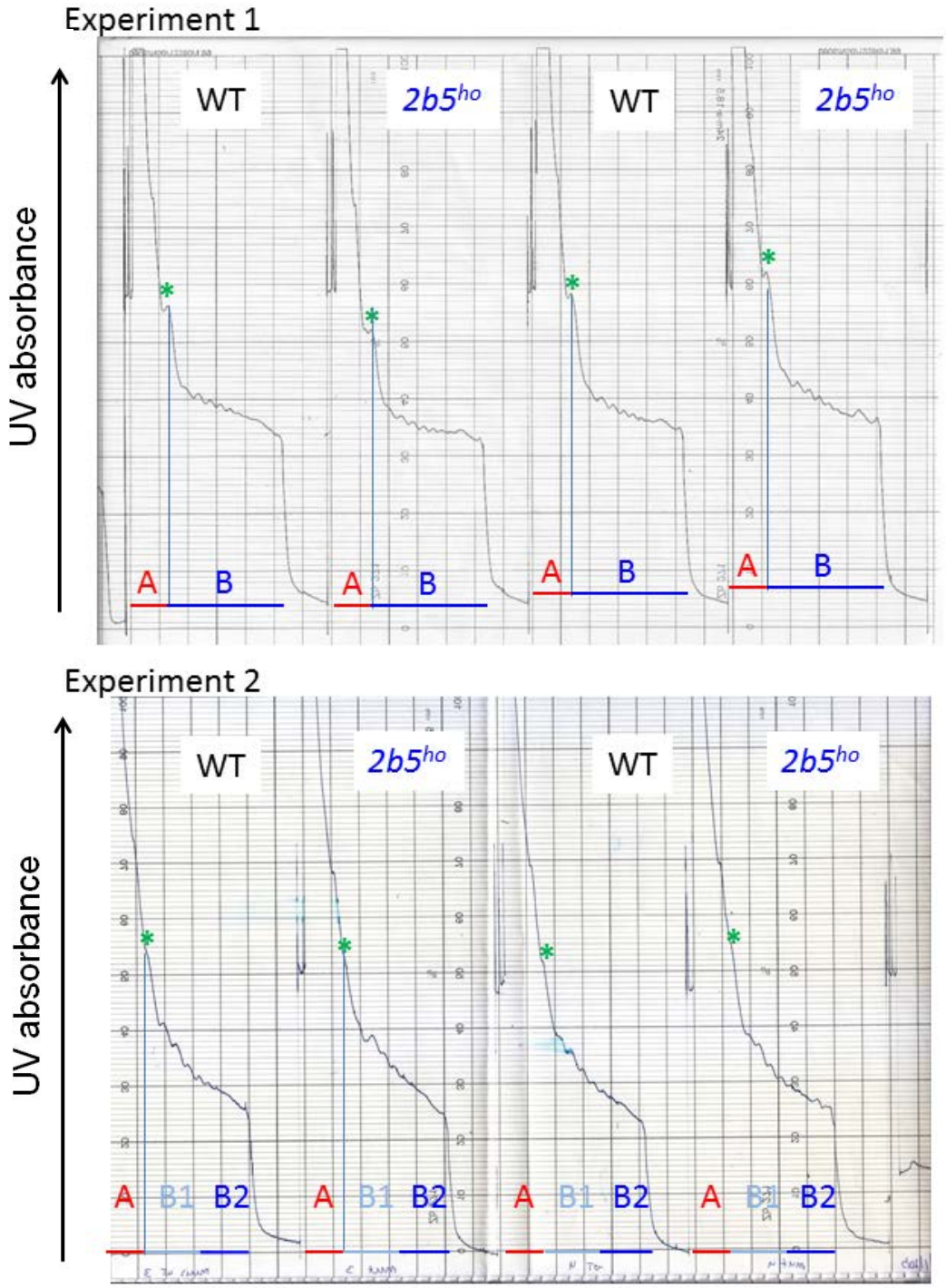

Supplementary Figure 1. Polysome profiles of wild type and *2b5^{ho}* mouse brain are similar. Sucrose gradients were pushed upwards by a 70% glycerol solution through an Uvicord with a velocity of 1 ml per min. UV absorbance was measured and was the basis for the fractionation. Mouse genotypes are indicated. *, 80S ribosome; A, monosome fraction; B, polysomes; B1, polysomes with less than five ribosomes per mRNA; B2, polysomes with 5 or more ribosomes per mRNA.

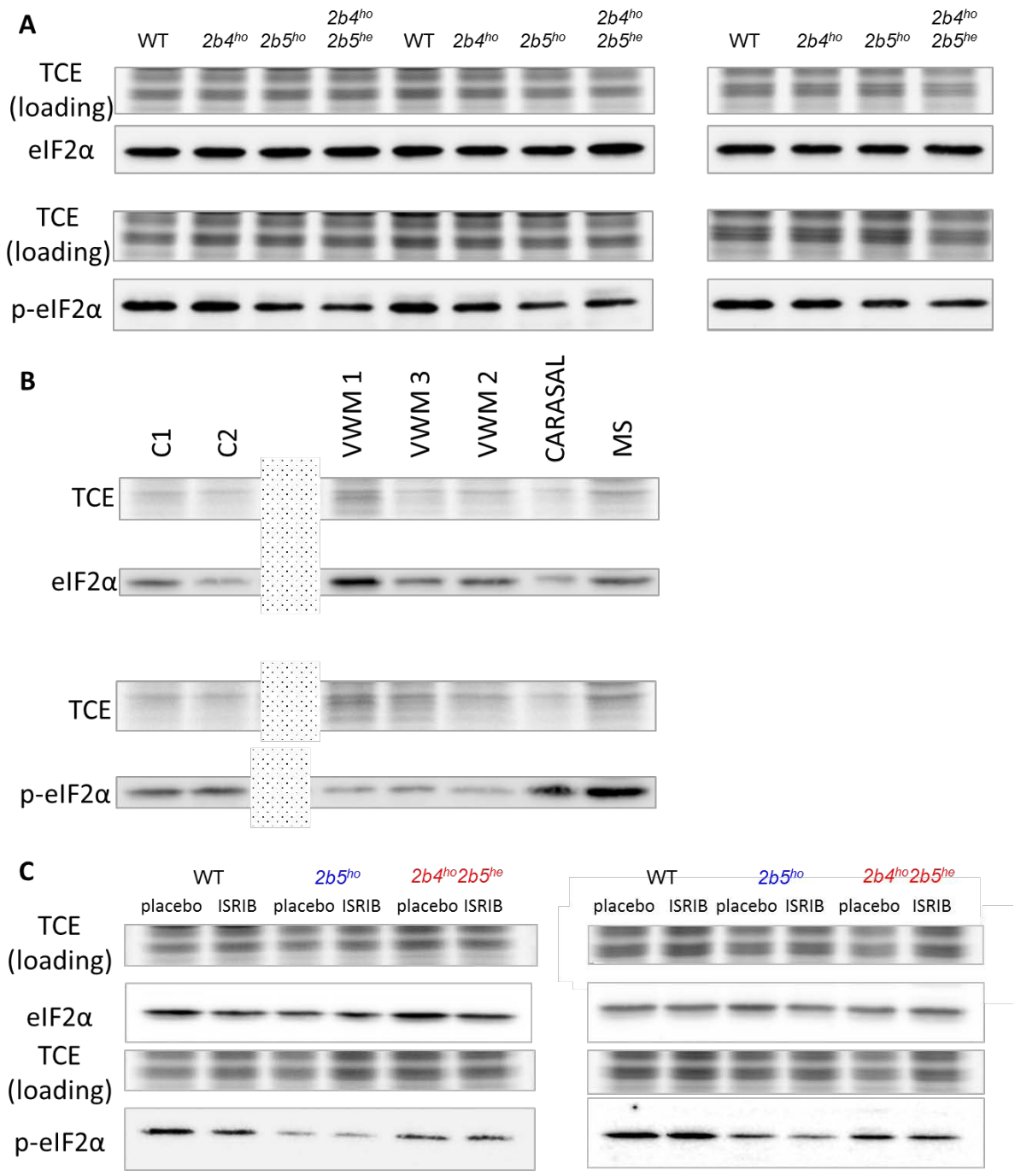

Supplementary Figure 2. Raw data for quantifying eIF2α phosphorylation using Western blot. Equal amounts of protein were applied to SDS-PAGE. In-gel protein loading and sample transfer was checked with 2,2,2-trichloroethanol (TCE). Quantitative results are shown in Fig. 1c (panel A), Fig. 1d (panel B) and Fig. 6A (panel C).

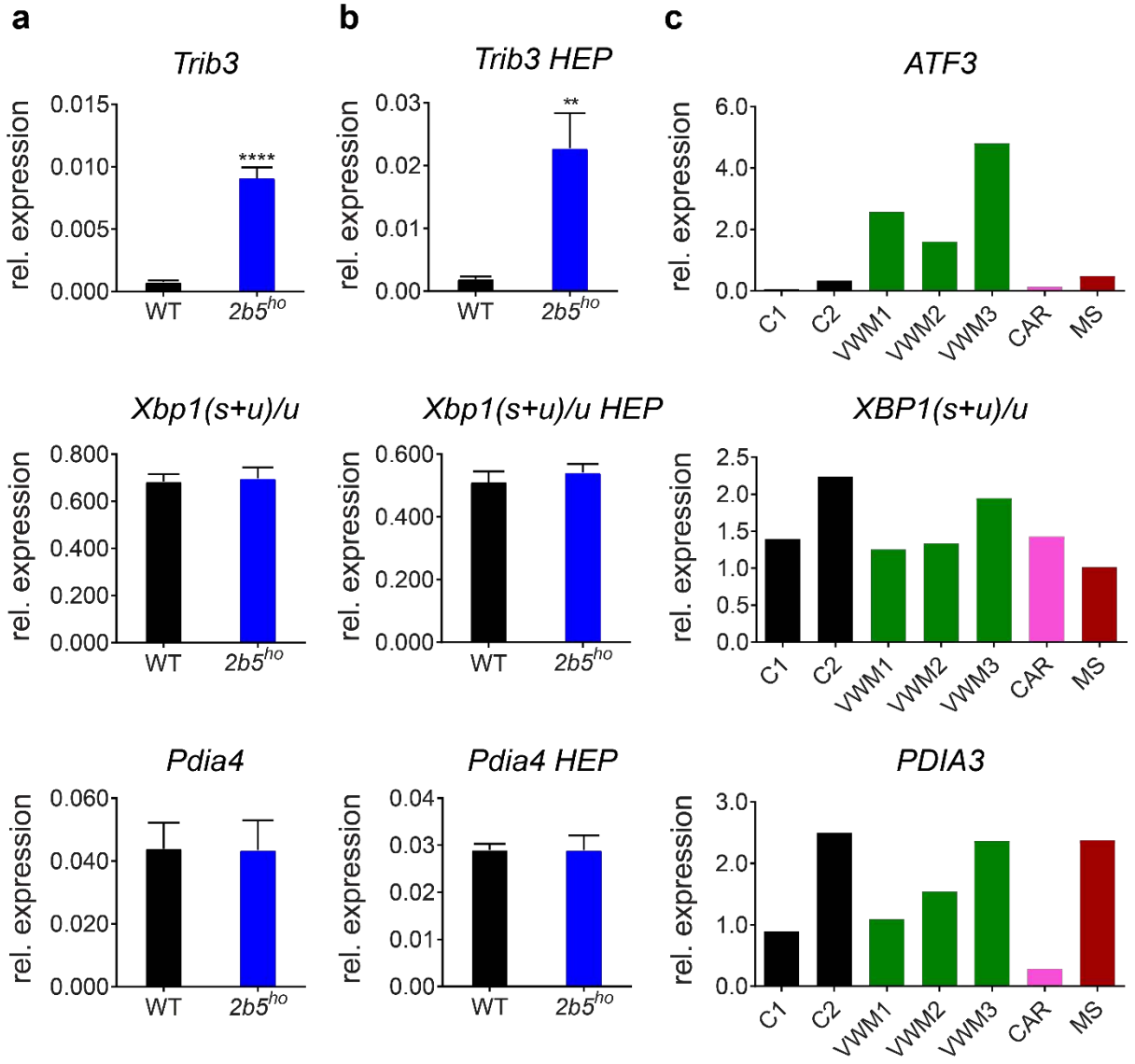

Supplementary Figure 3. The ATF4-transcriptome is expressed in VWM mouse and VWM patients' brain without markers indicating cellular stress. (**a**) mRNAs regulated by transcription factors ATF6 or IRE1α are similarly expressed in brains of 4-month-old WT and *2b5*^{ho} mice. *Pdia4* mRNA is regulated by ATF6 and *Xbp1* splicing (represented as *Xbp1(s+u)/u* ratio; s, spliced; u, unspliced) is regulated by IRE1α. *Trib3* was included as positive control for ATF4 regulation. (**b**) Similar expression levels were measured in brain of *2b5*^{ho} mice at humane end point (HEP). Graphs show average ± sd, n=6 for mRNA expression at 4 months (**a**) and n=3 at HEP (**b**). Comparisons between WT and *2b5*^{ho} samples are analyzed with Student's T-test. **p<0.01, ****p<0.0001. (**c**) mRNA levels were quantified in postmortem frontal white matter tissue from VWM patients and controls (negative controls without brain pathology, C1, C2 and disease controls CAR and MS; CAR, CARASAL; MS, multiple sclerosis, *GAPDH+AKT* was used as qPCR reference). *ATF3* expression is regulated by ATF4 (ISR marker). *PDIA3* expression by ATF6 and *XBP1s* (represented as *XBP1(s+u)/u* ratio) by IRE1α (ATF6 and IRE1α are UPR-specific markers). *PDIA4* was not detected in human brain tissue. Each bar represents one measurement (n=1). Details on control and patients' tissues are listed in Supplementary File 5.

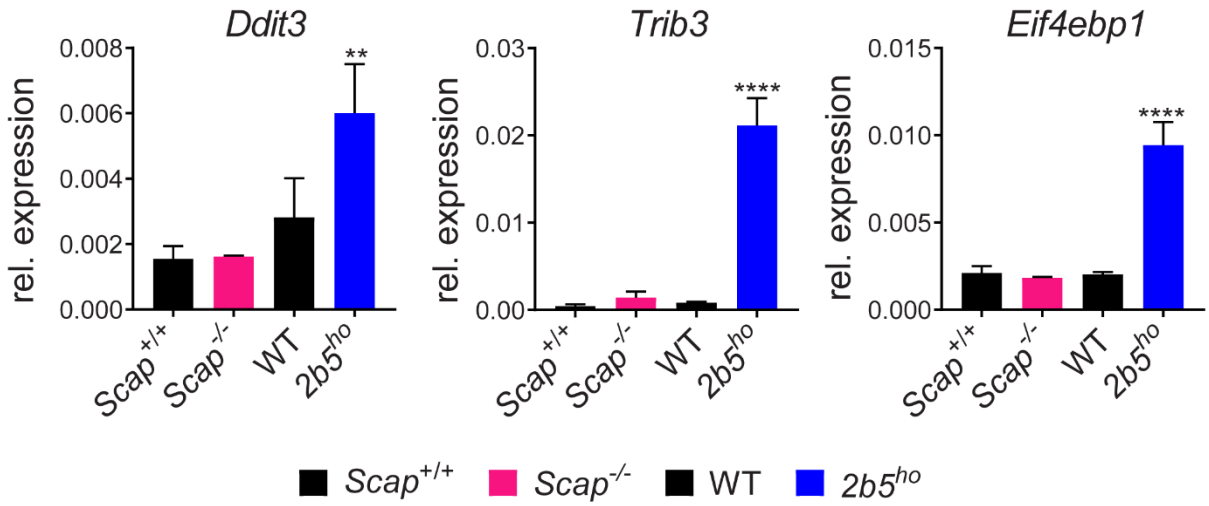

Supplementary Figure 4. Absence of enhanced expression of ATF4-regulated mRNAs in brain tissue from *Gfap-Scap*$^{-/-}$ mice. mRNA levels were determined with qPCR (*Gapdh+Akt* was used as qPCR reference). *Ddit3*, *Trib3* and *EIf4ebp1* mRNA expression was measured in forebrain tissue of 2-month-old *Gfap-Scap*$^{-/-}$ mice (mid-stage disease) and compared to *2b5*^{ho} mice (each mutant mouse line is compared to the isogenic control). Graphs show average ± sd, n=3. Statistical differences were determined using a Two-way ANOVA with Tukey's correction, **p<0.01, ****p<0.0001.

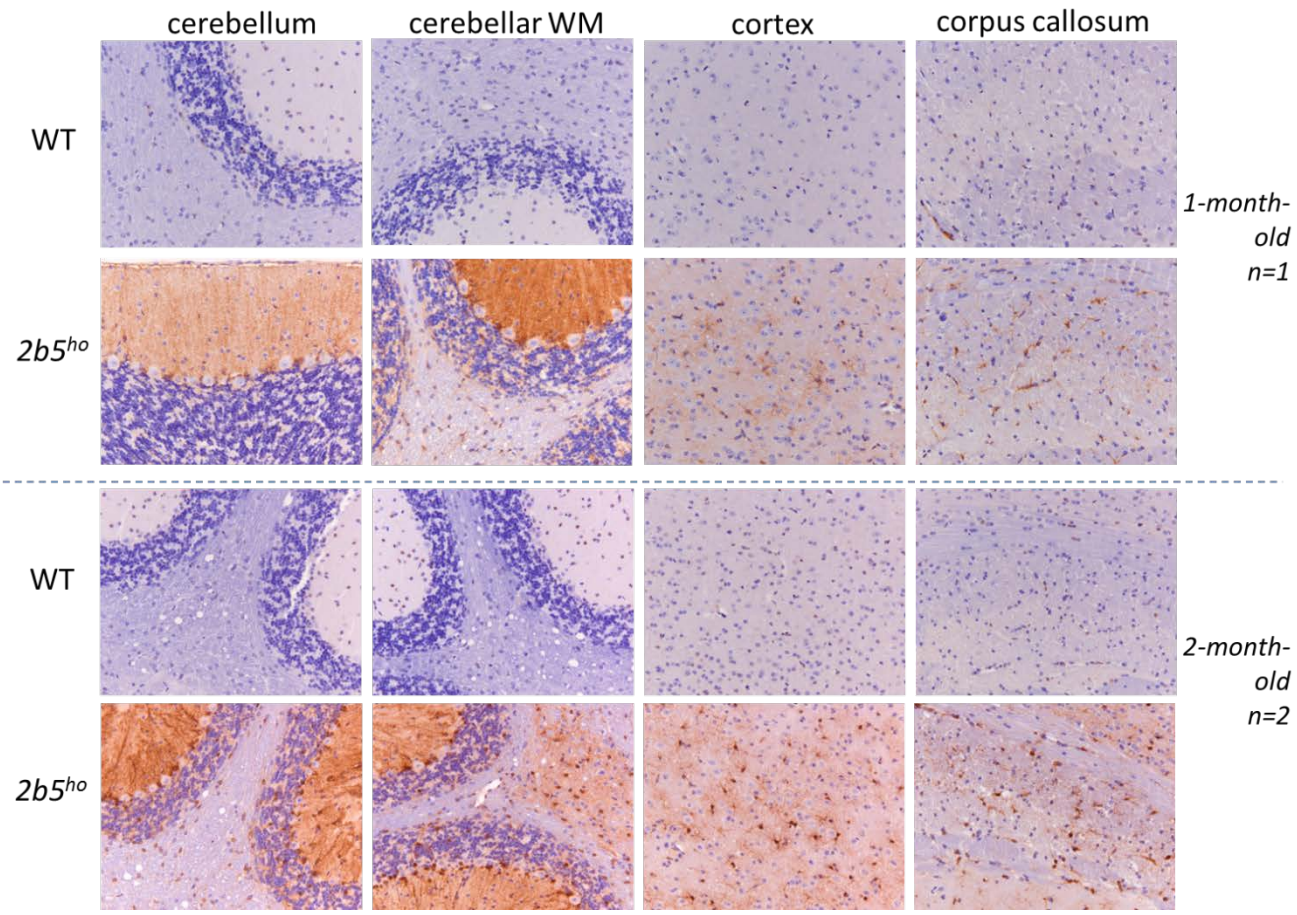

Supplementary Figure 5. White and grey matter astrocytes in VWM mice are immunoreactive for ATF4-regulated 4E-BP1 before clinical signs. 4E-BP1 immunoreactive cells (brown) are detected in white and grey matter macroglia of VWM mice. Sections from brain tissue from 1-month- and 2-month-old WT and *2b5*^{ho} mice were stained with antibodies against 4E-BP1. Findings in cerebellum, corpus callosum and cortex are indicated. Purple stain indicates nuclei.

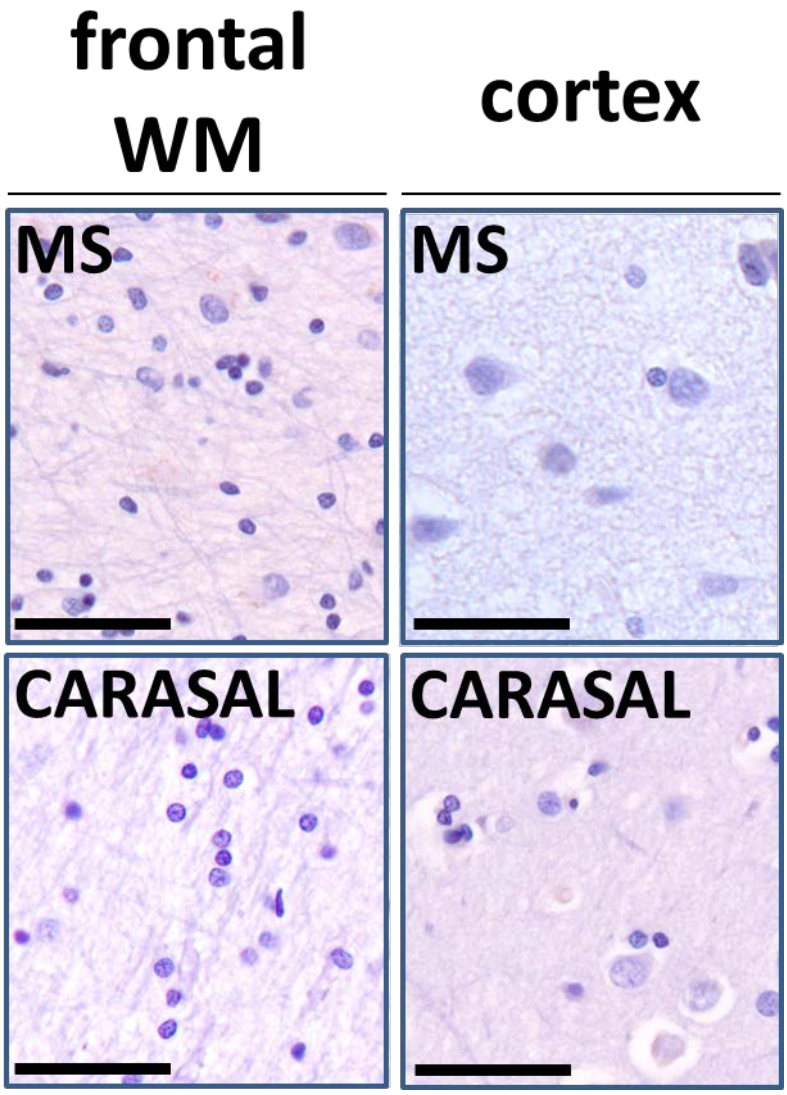

Supplementary Figure 6. Absence of 4E-BP1 immunoreactive astrocytes, oligodendrocytes or neurons in brain sections from MS and CARASAL patients. Sections were stained in parallel with the stainings shown in Figure 3 (2 sections per individual; 1 MS patient, 2 CARASAL patients were stained in total). Purple stain indicates nuclei. Black bar, 0.05mm.

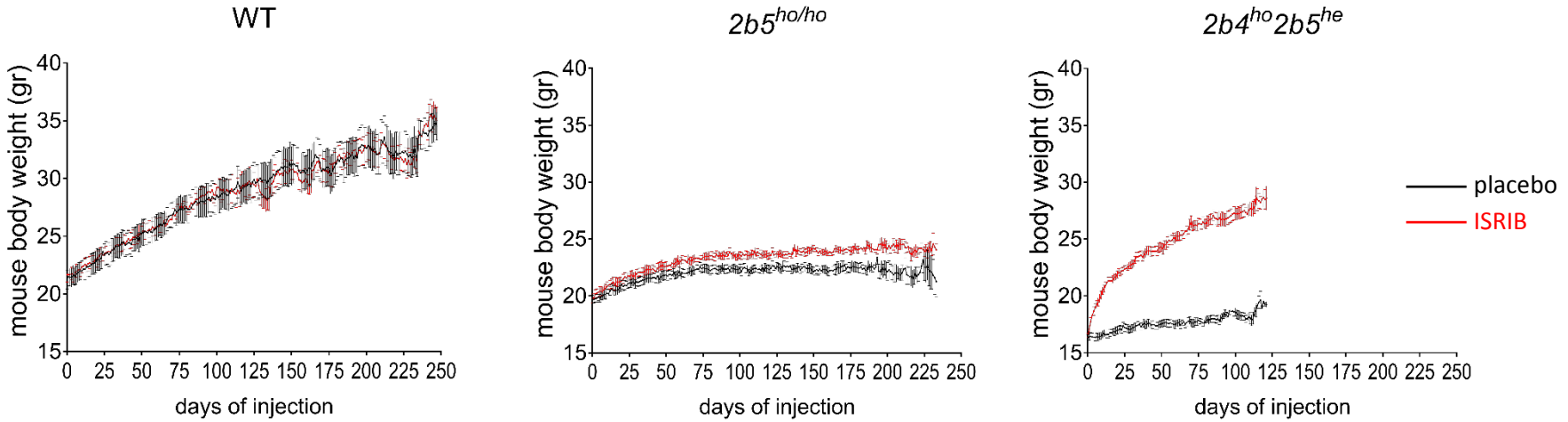

Supplementary Figure 7. ISRIB ameliorates reduced body weight in two VWM mouse models, most effectively in *2b4^{ho}2b5^{he}* mice. Graphs show body weight measures of placebo- and ISRIB-treated WT (n=6 per condition) and VWM mice (*2b5^{ho}* and *2b4^{ho}2b5^{he}* n=14 per condition or as indicated). Graphs show mean +/- SEM and are the same data as shown in Figure 5a, but now include SEMs that would obstruct the means in Figure 5a.

a

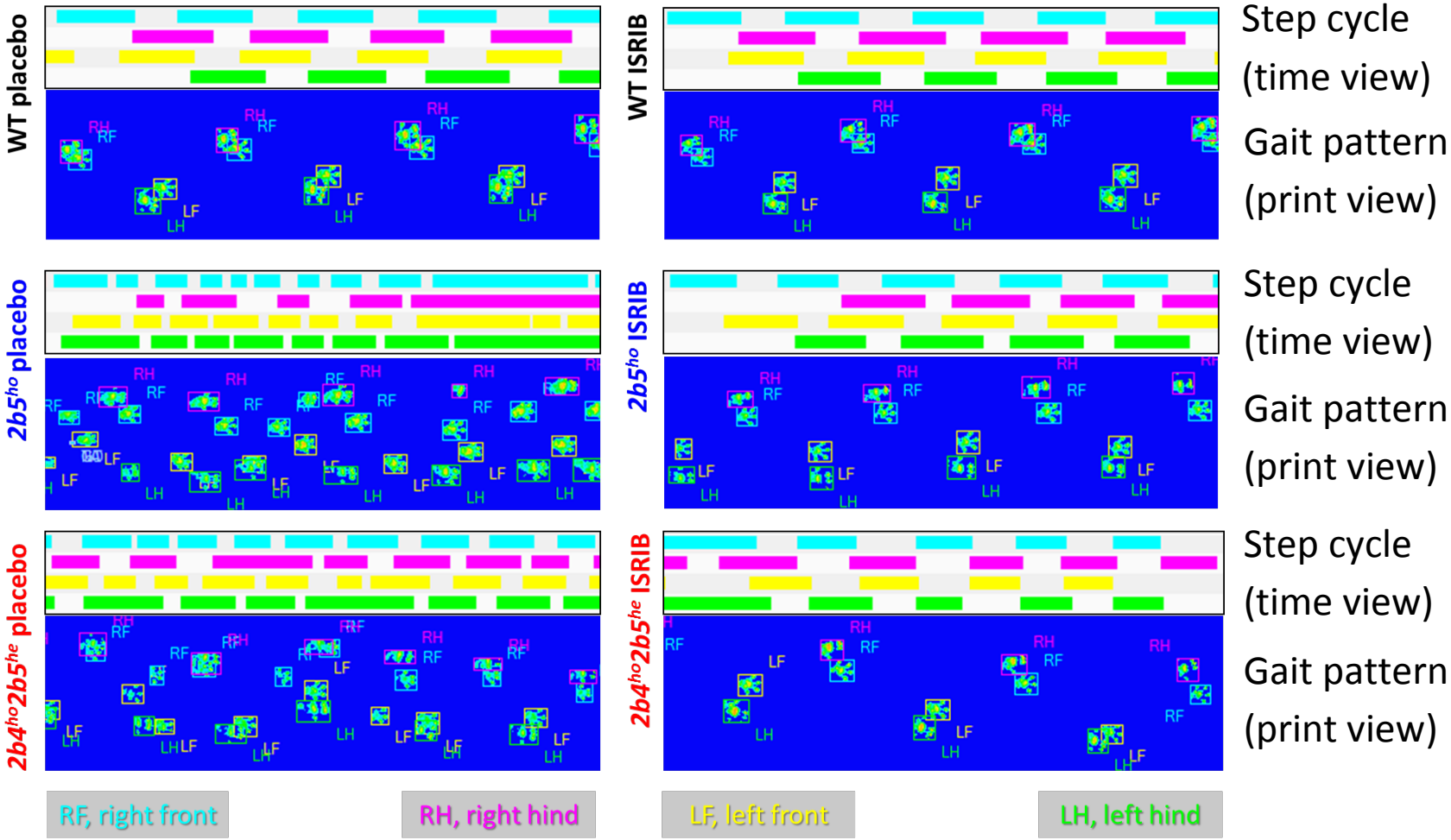
WT placebo
WT ISRIB
2b5ho placebo
2b5ho ISRIB
2b4ho2b5he placebo
2b4ho2b5he ISRIB
Step cycle (time view)
Gait pattern (print view)
Step cycle (time view)
Gait pattern (print view)
Step cycle (time view)
Gait pattern (print view)
RF, right front
RH, right hind
LF, left front
LH, left hind

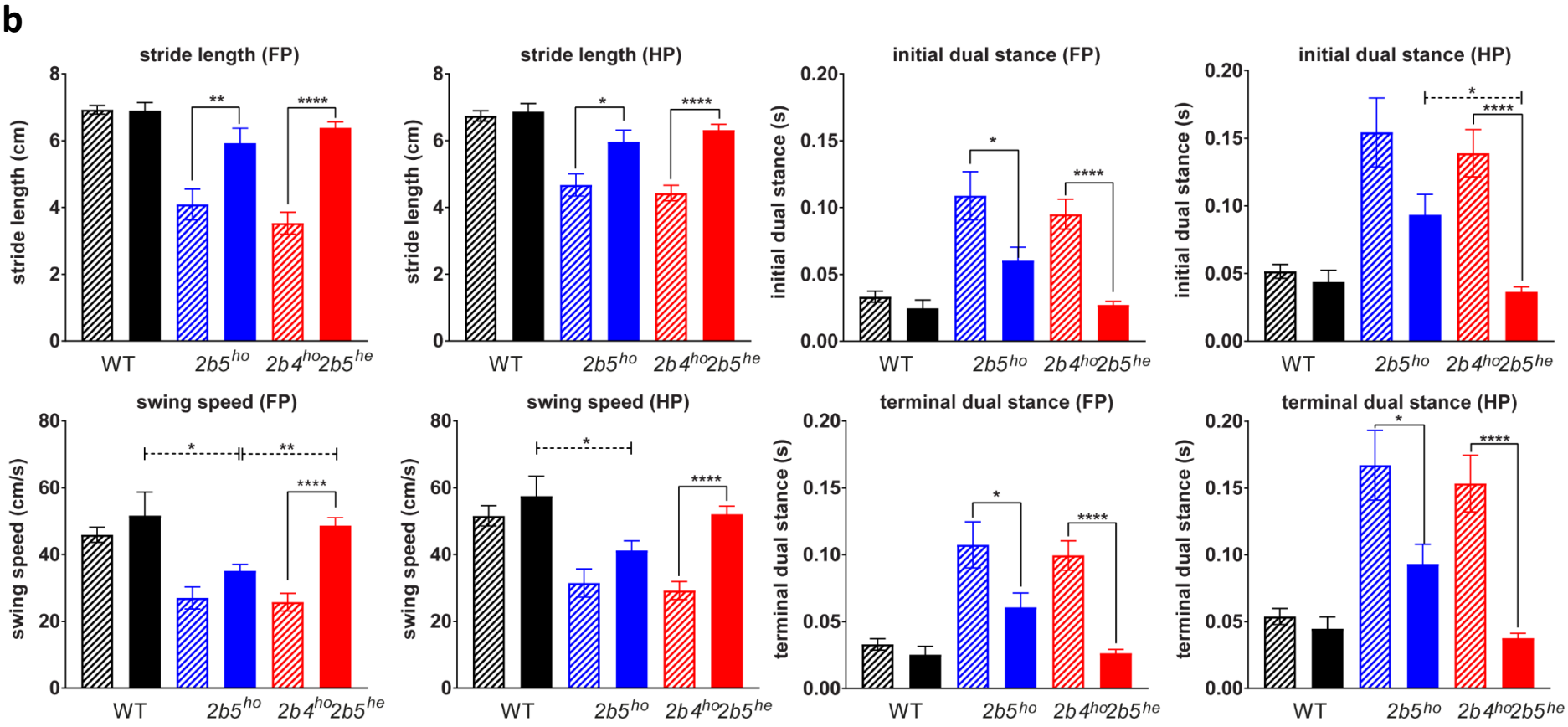

Supplementary Figure 8. (**a**) ISRIB ameliorates gait abnormalities in two VWM mouse models, most effectively in *2b4^{ho}2b5^{he}* mice; additional data of WT and VWM mice treated with placebo or ISRIB. Exemplary data on CatWalk for one mouse within each placebo- and ISRIB-treated group. Representative trace of the step cycle (time view, with colors indicating time that each paw is in contact with the glass plate) combined with the accompanying gait pattern (print view) are indicated. Genotypes and treatments are shown on the left-hand side (WT, black; *2b5^{ho}*, blue; *2b4^{ho}2b5^{he}*, red). (**b**) Each paw is color-coded as indicated below the traces. Additional quantified parameters from CatWalk tests not displayed in Figure 4. Error bars indicate SEM. Statistical analysis investigating the ISRIB differences within and among WT, *2b5^{ho}* and *2b4^{ho}2b5^{he}* was performed with a two-way ANOVA with Tukey's correction (Supplementary Data File 5). *p<0.05, **p<0.01, ***P<0.001, ****p<0.0001.

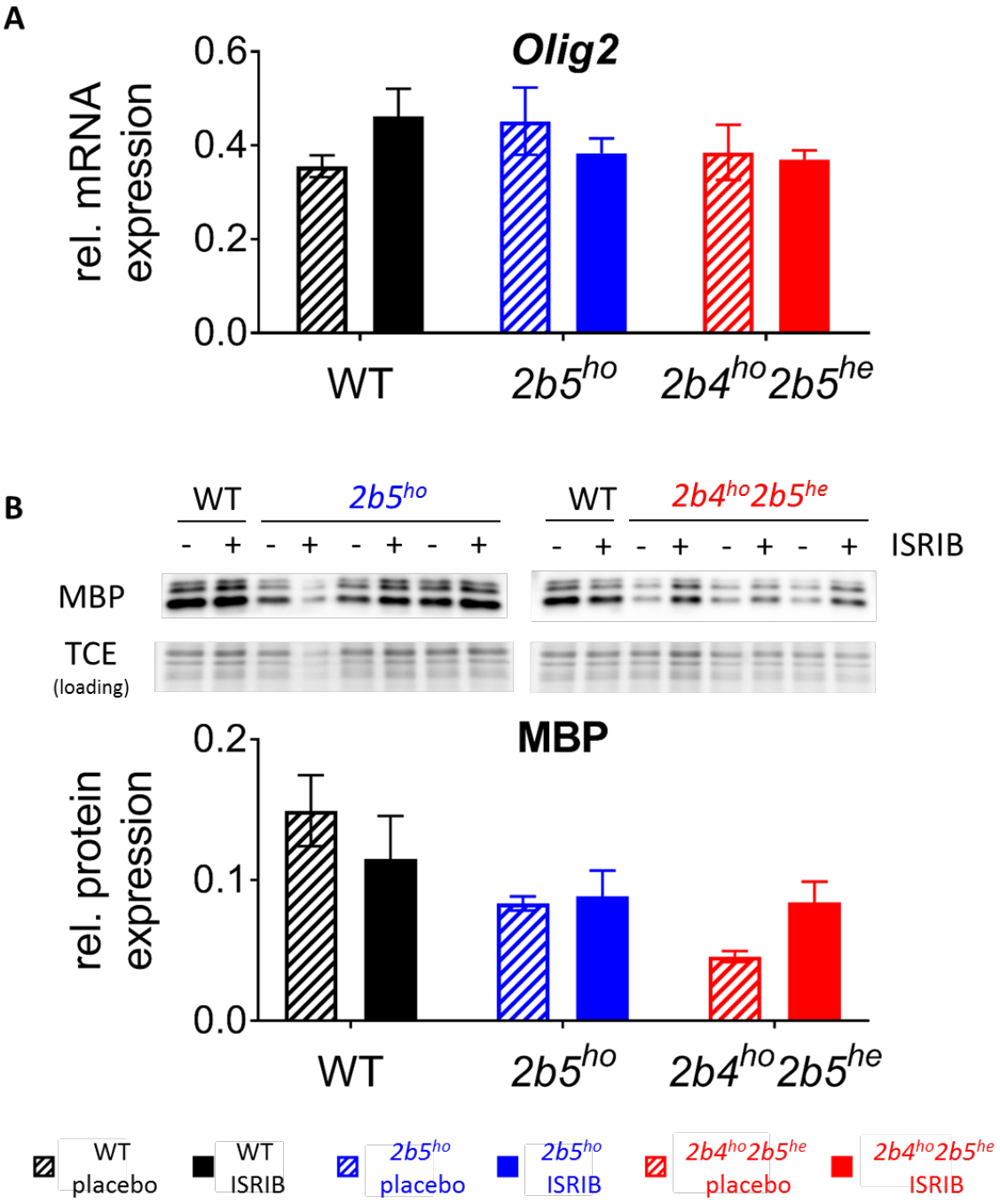

Supplementary Figure 9. Additional quantification of myelin markers by qPCR and Western blot. **A**, *Olig2* mRNA levels were determined with qPCR (*Gapdh+Akt* was used as qPCR reference; n=6 per group). *Olig2* mRNA is expressed in oligodendrocytes independent of their maturation. Graphs show average ± sd, n=3. **B**, MBP protein levels were investigated with immunoblotting. Equal amounts of protein were applied to SDS-PAGE. In-gel protein loading and sample transfer was checked with 2,2,2-trichloroethanol TCE). MOG protein levels were also investigated, but yielded immunosignals out of the linear range, making Western blot unsuitable for quantification. Statistical differences for ISRIB effects were not found using a Two-way ANOVA with Tukey's correction. MBP protein levels in placebo-treated *2b4^{ho}2b5^{he}* mice were statistically different from MBP proteins levels in placebo-treated WT mice (p=0.0204).

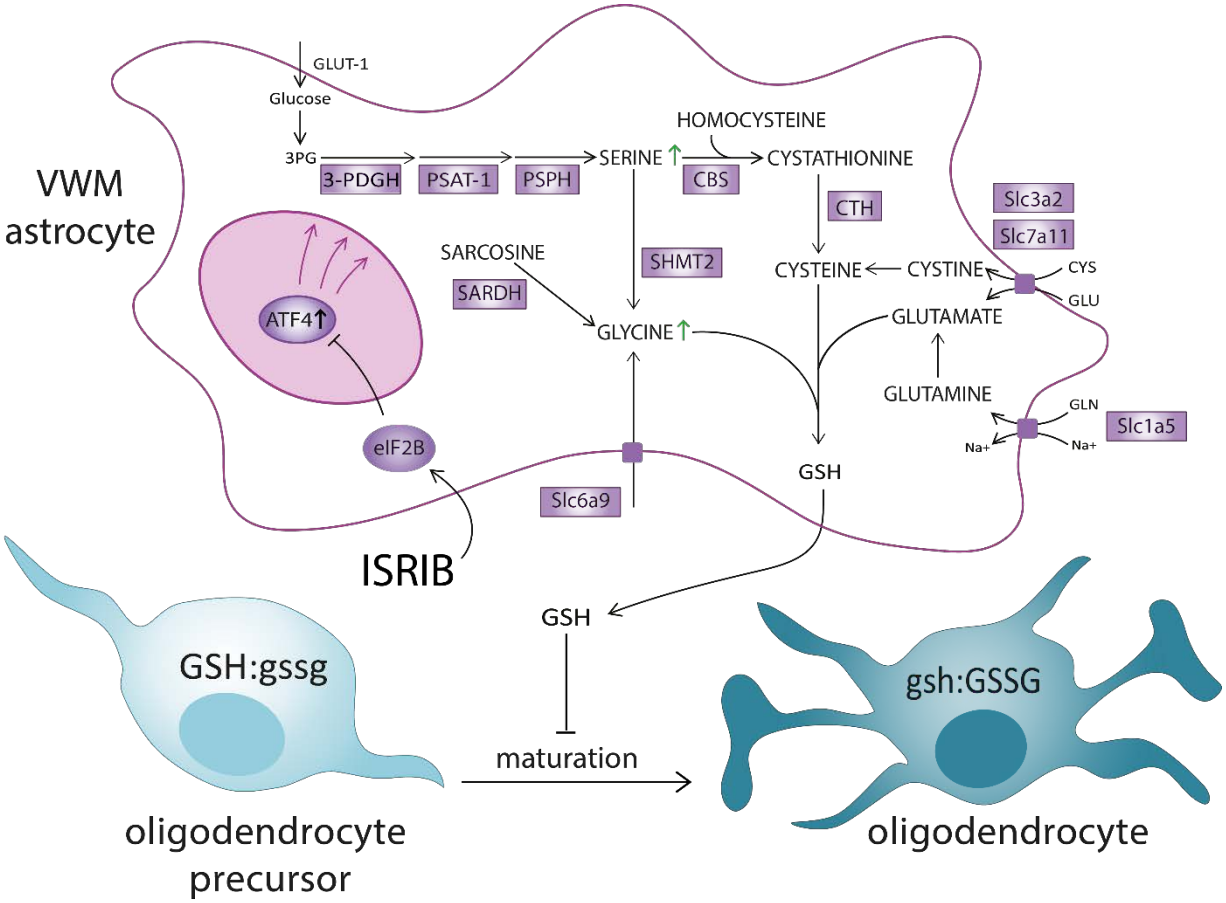

Supplementary Figure 10. Molecular model for failing oligodendrocyte maturation in VWM and molecular effects of ISRIB. ISR-deregulation in VWM astrocytes increases ATF4, which regulates expression of mRNAs (indicated are upregulated mRNAs in magenta-shaded boxes). The ATF4-regulated transcriptome in VWM astrocytes affects amino acid metabolism, serine biosynthesis and glycine metabolic processes resulting in increased levels of the reducing compound glutathione (GSH). GSSG:GSH indicates redox potential (oxidized:reduced glutathione), with capitalized font indicating the most abundant type of glutathione (GSH, reduced; GSSG, oxidized). GSH may induce a reductive shift in redox potential interfering with maturation of oligodendrocyte precursors (OPC) to mature oligodendrocytes. The resulting reductive change in redox status could inhibit oligodendrocyte maturation, a process known to be driven by oxidative shifts in redox potential. Increased levels of serine and glycine (indicated with green arrows) have been described in cerebrospinal fluid from VWM patients. ISRIB impacts eIF2B activity and reduces ATF4 expression, consequently expecting to influence redox potential and improve OPC maturation.